

Source: Motorola
Title: Spatial Channel Model, Fading, Propagation Models and Verification
Document for: Discussion

1. SUMMARY

This contribution investigates the fading behavior when the spatial channel model components are time-evolved. These effects are examined and compared using the autocorrelation function.

A refinement to the propagation model for the SCM Micro-cell is proposed. The suggested approach is to use the Cost-231 Walfish-Ikegami model for both the non-line-of-sight and if used, the line-of-sight cases. Some questions remain on selecting the parameter values relating to the composite angle spread.

2. FADING BEHAVIOR

In [1] the performance of the fading behavior was considered where the calculation of correlation was described and used to compare a number of alternatives. Small differences were seen in the correlation shown for most cases.

In the following discussion, the issue of fading for the spatial channel model, with a specific angle spread is further characterized. In general, the main difference in the SCM compared to classical fading models is that the angle spread is not uniform, but narrow, e.g. $\sigma_{AS} = 35^\circ$, which limits directions of arrival of the scattered sub-components. This reduced angle spread, which is based on a variety of measurements, affects the correlation behavior of the fading model resulting in an increased correlation distance. This increased correlation, which is a function of the AoA, reduces the effective speed of the fading process. The Rayleigh fading distribution is not affected, i.e. the probability of a given fade depth remains the same.

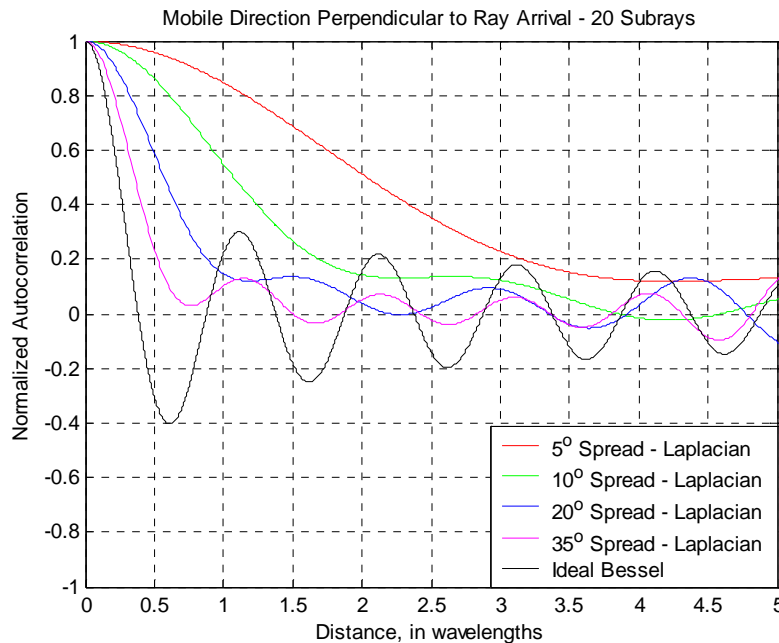


Figure 1, Fading Autocorrelation, Narrow Angle Spreads at 90° to UE path

Figure 1 describes the unique behavior of the fading autocorrelation when the subscriber is traveling perpendicular to the average direction of sub-ray arrivals. The value of angle spread for the subscriber, $\sigma_{AS} = 35^\circ$ is shown along with some narrower spreads so that the trend can be seen.

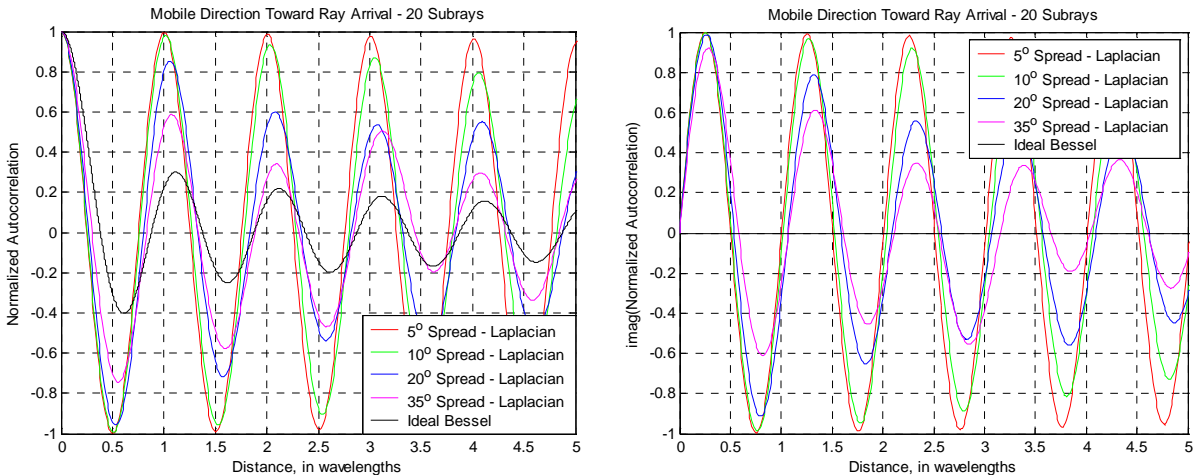


Figure 2a (Real) Angle Spreads at 0° to UE path Figure 2b (Imag) Angle Spreads at 0° to UE path

Figure 2a & 2b illustrate the effect of changing the orientation of travel so that the subscriber is traveling in the direction toward the incoming sub-rays. In this example, the subscriber angle spread of $\sigma_{AS} = 35^\circ$ is shown along with some narrower spreads so that the trend can be seen. Notice that the ideal Bessel function is real-valued, and remains the same because it is characterized by uniform arrivals. For narrow spreads however, the autocorrelation has increased in magnitude and is complex valued where the magnitude follows the rate of decay that is observed. The increase in correlation is explained by the Doppler shifts between the paths now being very similar when the angles of arrival of the sub-rays are distributed over such a small range as shown in these examples.

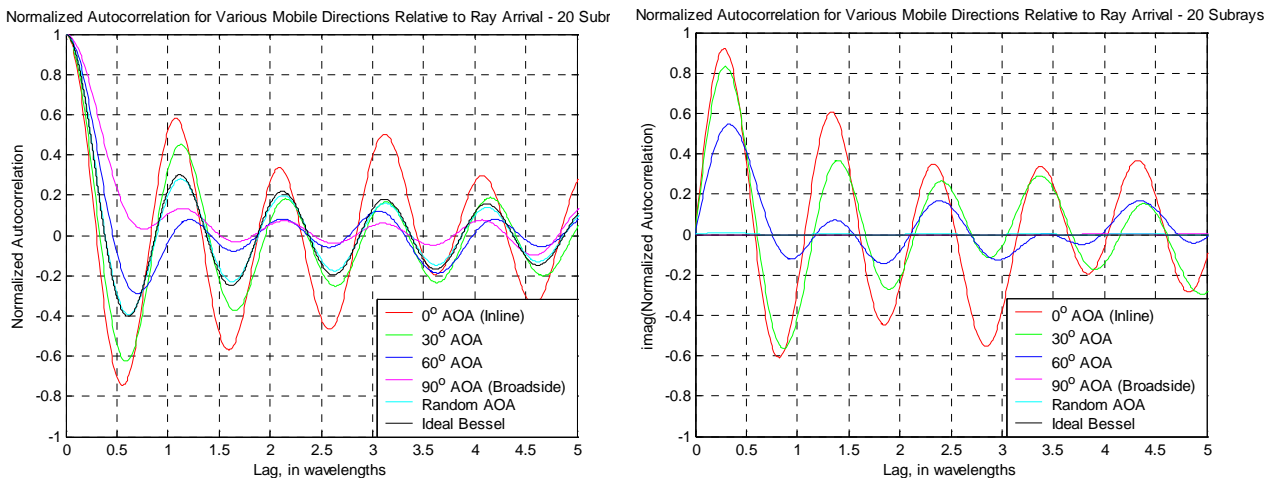


Figure 3a (Real) $\sigma_{AS}=35^\circ$ with various AoAs Figure 3b (Imag) $\sigma_{AS}=35^\circ$ with various AoAs

Figure 3a & b describe the effect of different angles of arrival for an angle spread of $\sigma_{AS} = 35^\circ$. For the case of AoAs = 0° , 30° , and 60° , the Autocorrelation is complex valued. Also included is the case where the angle of arrival is chosen randomly from a uniform distribution for a variety of

sample segments. The resulting behavior of the autocorrelation is real-valued and very close to the ideal Bessel function, which is shown for comparison. This indicates that fading produced by the narrow angle spread, which is sampled from various AoAs, produces a composite behavior that matches the ideal as expected.

2.1 Comparison of different fading models

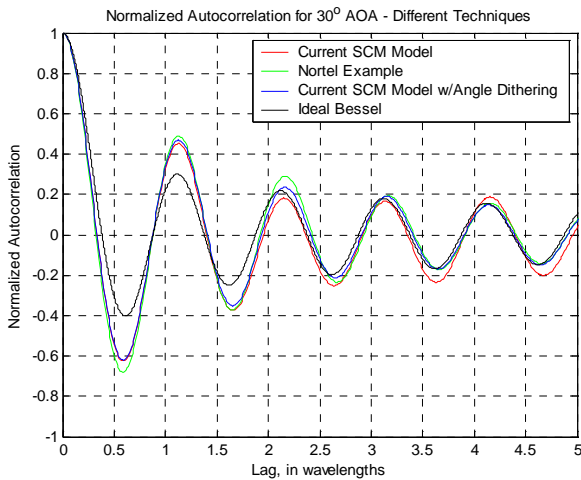


Figure 4a, (Real) $\sigma_{AS}=35^\circ$ AoA=30°

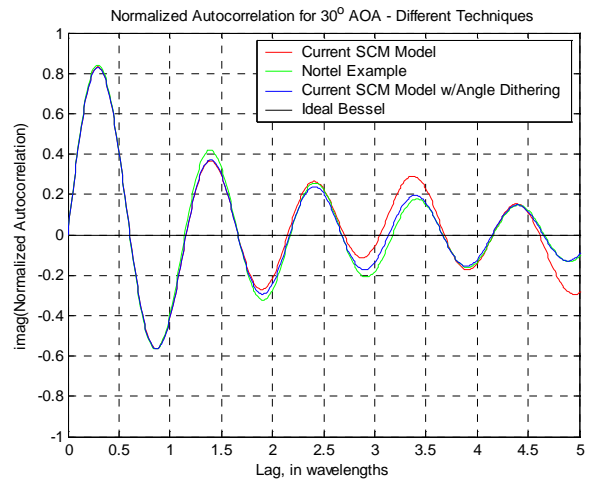


Figure 4a, (Imag) $\sigma_{AS}=35^\circ$ AoA=30°

Figures 4-6 considers three different variations to the fading model to examine the differences in performance. In the figures the fading is simulated for an angle spread $\sigma_{AS}=35^\circ$. The following cases are plotted in the figures:

- a.) The SCM model with 20 sub-ray of equal power and with $\sigma_{AS} = 35^\circ$
- b.) The Nortel example[1] is shown where an equal angle spacing is used with a Laplacian power per sub-ray. The angles are randomly perturbed by a uniform distribution within a bin around each sub-ray, and the powers are correspondingly set with a Laplacian envelope according to the angles that were used.
- c.) This example uses the SCM model with 20 equal power sub-rays, but includes a uniform randomizing of each of the angles within a bin around each sub-ray. The powers remain constant.
- d.) Ideal Bessel Function.

Figure 4 compares the correlation for the different techniques when the AoA=30°. Other AoAs produce different responses as already shown. In this experiment, the correlation values for models a, b, and c, are complex valued, and appear to be relatively similar.

In order to examine the differences more carefully, the data in Figure 4 is shown as a magnitude plot in Figure 5. From this figure, it is observed that the three techniques are similar with the undithered SCM model having more variation at large lag times, however it produces a better match to ideal[2] at the important subscriber spacing of $\lambda/2$. This model also does relatively good across the various AoAs that were compared (some not shown), 0°, 30°, 60°, and 90°. It should be noted that the variations will be different for every AoA, but when averaging over the AoAs, the result is a good match to the ideal as shown below.

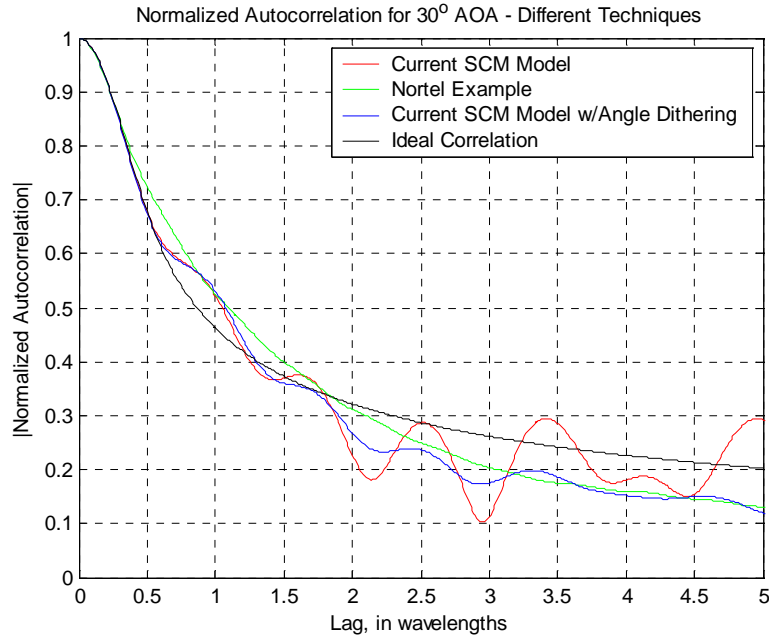


Figure 5, Autocorrelation (Magnitude), $\sigma_{AS}=35^\circ$, $AoA=30^\circ$ with different sub-ray configurations

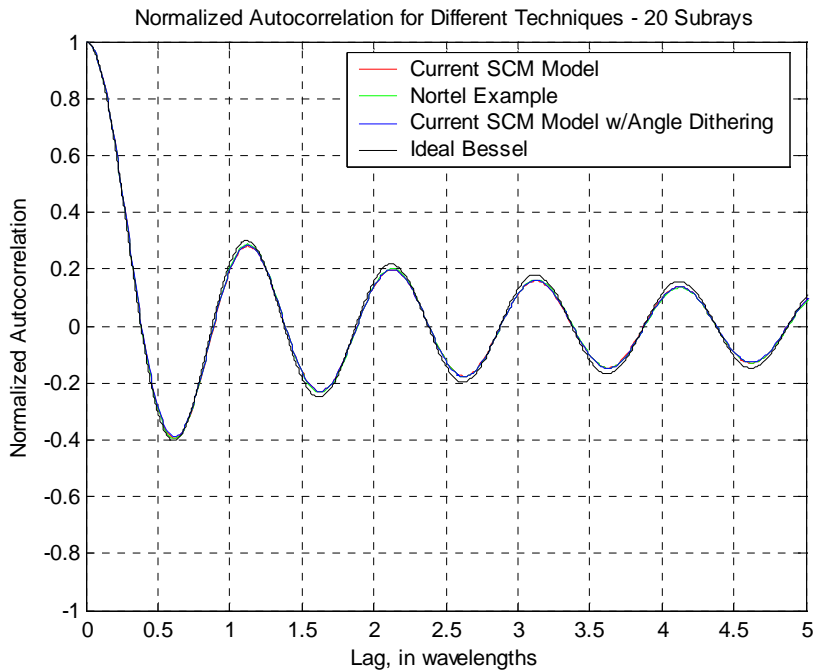


Figure 6, Fading Autocorrelation, $\sigma_{AS}=35^\circ$, $AoA=Random$, with different sub-ray configurations

Figure 6 illustrates the case where models a, b, & c, are evaluated with random AoA for each sampling interval. The results are all real-valued and indicate that the current SCM model, or models with additional randomization in angle or power are all comparable and produce a sufficiently good match to the ideal Bessel function when evaluated across the various possible angles of arrival.

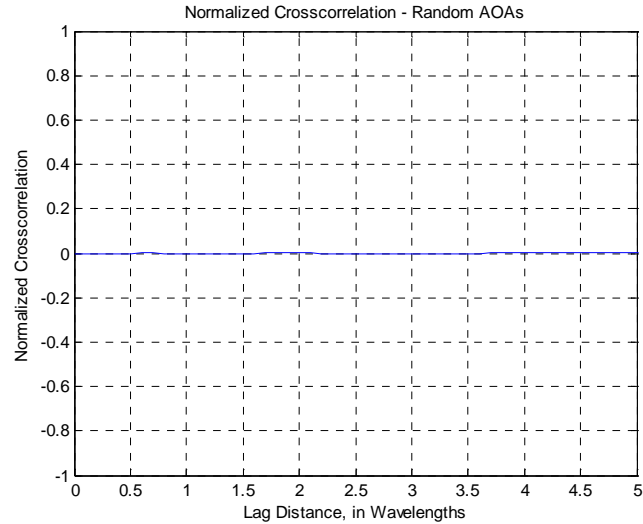


Figure 7, $\sigma_{AS}=35^\circ$, UE orientation = Random

Figure 7 illustrates the crosscorrelation between two fading signals, and shows that the cross correlation is essentially zero as expected. For this experiment random subscriber orientations were selected, and the AoAs of the two signals varied based on a cellular geometry which encompassed a wide range of possible angle differences. The per-path AS = 35° , and the orientation and AoAs were randomized after each interval, for a large number of trials.

3. MICRO-CELL PROPAGATION MODELS

3.1 Path Loss Model

After some investigation into possible path loss models for urban micro-cells, it was observed that the COST 231 Walfish-Ikegami[3] model produces path loss slopes (38 dB/dec*) that are more generally comparable to measurements than Feuerstein[4] (slope = 26 dB/dec**), which seemed to have a limited number of points at shorter distances. Also, given its previous use as a GSM model, it would be a reasonable model to use for micro-cell path loss.

The actual Walfish-Ikegami model is a function of orientation to the street grid since the diffraction loss over the last building is affected by the orientation. The result is a change in intercept as a function of angle between the base to mobile path and the street, whereas the slope does not change with orientation.

For the purposes of modeling a micro-cell scenario as a number of hexagons, it would be useful to select an orientation to produce an average intercept, instead of it varying across the small hexagon. Allowing it to vary would produce a bias across the cell resulting in different path losses at one edge of a 120 degree sector compared to the other by as much as 14dB. Thus it creates a significant non-uniformity, making it difficult to interpret what happens in the small hexagon. For reasons of simplicity, the average value would be reasonable since the model would have a log normal shadow fading component as well.

*For the parameters given below, Walfish-Ikegami NLOS slope = 38dB/dec.

**For the Feuerstein model, the NLOS slope = 26 dB/dec.

3.2 Angle Spread Model

From [5], measurements indicate that the angle spread for urban micro-cells can be dramatically different for LOS and NLOS scenarios where the median value ranges from 7.5° to 19° respectively in the measurements described. The composite AS of the current model being discussed in the SCM has a mean value of 11.7° , which would indicate that it is more heavily weighted toward the LOS condition. It would appear reasonable to separate the LOS and NLOS for the propagation loss and the angle spread distributions, which would match the cases presented in [5].

To obtain these resulting AS distributions, some adjustment will be required to the parameters describing the three paths (before normalization). Figure 8a shows the effect on AS for different values of the log normal randomizing noise used in the setting the micro-cell powers.

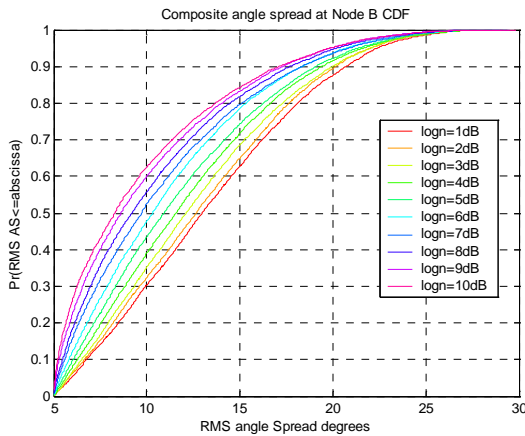


Figure 8 a, Composite AS for U(-30, 30)

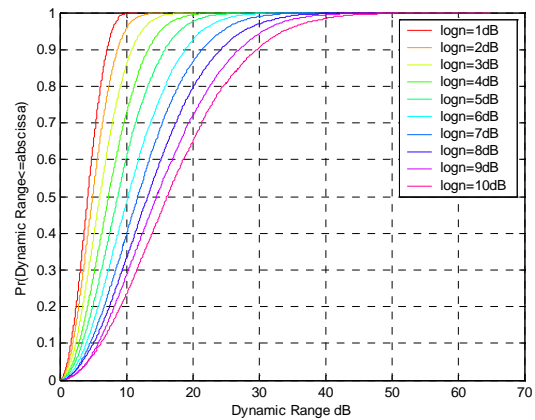


Figure 8 b, Dynamic range for U(-30, 30)

From Figure 8a, it is seen that a median value of 19 degrees is not possible when distributing the paths uniformly from -30 to $+30^\circ$. Notice that the randomizing noise sigma also affects the dynamic range experienced by the three ray powers as shown in Figure 8b.

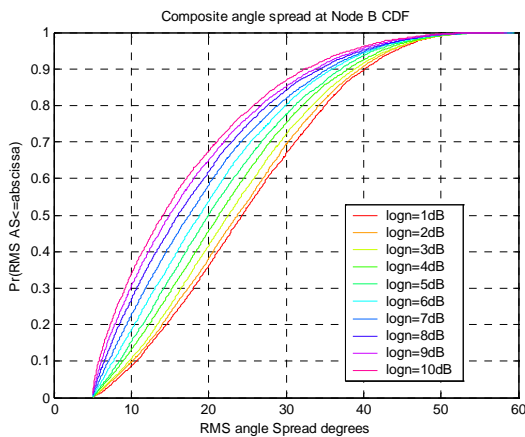


Figure 9 a, Composite AS for U(-60, 60)

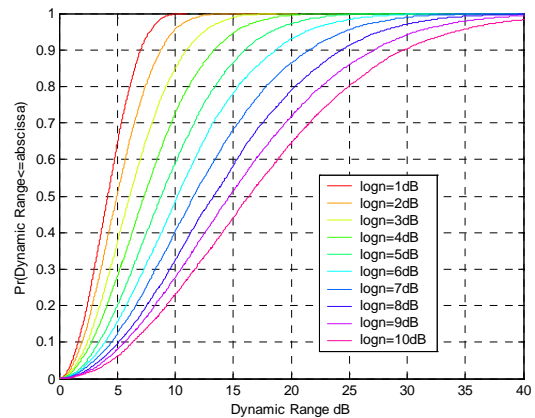


Figure 9 b, Dynamic range for U(-60, 60)

In order to select the ray powers so that a reasonable dynamic range is produced, such as 20dB for 2% of the channel draws, a sigma of around 5dB is required. This matches the most recent proposal[6], and appears to be a suitable value. With this constraint, the angle distribution must be

increased to roughly $U(-60, 60)$ to produce an angle spread with a median of 19° when the log normal component is 5dB. See Figure 9a&b. This value of AoA is significantly higher than the previously proposed model, however it would seem reasonable given a rooftop antenna installation.

For simplification purposes, it may be best to model only NLOS paths. To select a mix of LOS and NLOS, additional rules will be needed for choosing the percentage of the time for each occurrence, such as selecting LOS more often when close to the base. When selected to be LOS, the path loss, AS distribution, Rician K-factor, Log Normal Shadow fading, and possibly the delay spread would need to be set accordingly.

3.3 Proposed Micro-cell Path Loss Model

NLOS: Walfish-Ikagami,

Building = 12m Building to building distance = 50m

Antenna = 12.5m Street width = 25m

mobile = 1.5m Orientation = 30 deg for all paths (produces an average value of intercept)

Resulting Slope = 38dB/dec Resulting Intercept = 150 dB

AS model = 19 deg median (from COST259[5], p. 163)

Log Normal Shadow Fading = 10dB sigma

Cell Radius = 400m

K-factor = 0 dB

For LOS: (optional) Walfish-Ikagami street canyon equation,

$L = 42.6 + 26\log_{10}(d) + 20\log_{10}(f_c)$ d in Km, f_c in MHz.

AS = 7.5 deg median (from COST259[5], p. 163)

Log Normal Shadow Fading = 5-7 dB sigma

Cell Radius = 400m

K-factor = function of radius, TBD

MIX: LOS & NLOS

Rules needed.

4. CONCLUSION

In this contribution an investigation into the fading behaviors of the SCM model was made which included the effects of narrow angle spread, and angle of arrival. Three different sub-ray generation techniques were compared. The results of angle dithering and combinations of angle and power dithering produce smoother autocorrelation functions, but no better results after averaging over AoAs.

The results showed that a sufficiently good match was obtained to the ideal Bessel function when the fading was evaluated across the various possible angles of arrival.

The path loss model was investigated, and a simplified version of Walfish-Ikegami was proposed for the Urban Micro-cell scenario.

The AS for the Urban Micro-cell has values that are dramatically different for LOS and NLOS scenarios where the median value ranges from 7.5° to 19° respectively as described in [3].

NLOS and LOS considerations affect the micro-cell propagation model as well as many other parameters. Thus for simplicity perhaps the micro-cell models should be limited to NLOS paths.

5. REFERENCES

- [1] Nortel Networks, "SCM Model Correlations," SCM-065_v2, Teleconference, October 10th, 2002.
- [2] J. Salz and J. H. Winters, "Effect of Fading Correlation on Adaptive Arrays in Digital Mobile Radio," IEEE Tr. on Veh. Tech., Vol. 43, No. 4, pp. 1049-1057, November 1994.
- [3] COST 231 Final Report, "Digital mobile radio: COST 231 view on the evolution towards 3rd generation systems". Editors: Damosso, E. and Correia L.M., European Commission – COST Telecommunications, Brussels, Belgium, 1998.
- [4] M. J. Feuerstein, K. L. Blackard, T. S. Rappaport, S. Y. Seidel, and H. H. Xia. Path loss, delay spread, and outage models as functions of antenna height for microcellular system design. IEEE Transactions on Vehicular Technology, vol. VT-43, no. 3, pp. 487-498, 1994.
- [5] L. M. Correia, Wireless Flexible Personalized Communications, COST 259: European Cooperation in Mobile Radio Research, Chichester: John Wiley & Sons, 2001.
- [6] Lucent, "System model verification and calibration", SCM-069R2, Conference call, November 21, 2002.

Notice

©2002 Third Generation Partnership Project Two (3GPP2). All rights reserved. Permission is granted for copying, reproducing, or duplicating this document only for the legitimate purposes of 3GPP2 and its organizational partners. No other copying, reproduction, or distribution is permitted.

Copyright Notification

No part may be reproduced except as authorized by written permission.
The copyright and the foregoing restriction extend to reproduction in all media.

© 2002, 3GPP Organizational Partners (ARIB, CWTS, ETSI, T1, TTA, TTC).
All rights reserved.